

Performance of Composite Outdoor Insulator Under Superimposed Direct and Switching Impulse Voltages

Davide Pinzan , Fabio Branco , Manu A. Haddad , Mohammed El Amine Slama , Maurizio Albano , Ronald T. Waters , and Helder Leite 

Abstract—High Voltage Direct Current (HVDC) systems are increasingly being adopted around the world to integrate renewable resources, increase power transfer, and allow flexible grid operation. HVDC overhead lines play a critical role in this, and focus is needed on the research of composite outdoor insulators failure. In the case of a pole to ground fault of a bipolar scheme, the healthy pole experiences a slow transient overvoltage similar to a Switching Impulse (SI) superimposed on the operational DC voltage. However, there is no standard test for such voltage superimposition. This paper investigates the performance of a composite insulator stressed with such superimposition under dry and rain conditions. To determine the direct voltage influence on the flashover voltage, the results have been compared with the SI only case. Four different rain conductivities have been used in the test program because these insulators can be exposed to different acid conductive rain types, typical of industrialized environments. Both vertical and horizontal orientations have been studied. It was possible to conclude that, in most cases, the direct voltage pre-energization has a negative impact on the flashover performance. The increase in rain conductivity leads to lower flashover values, and the horizontal orientation outperforms the vertical configuration. Under these test conditions, the flashover voltages were all larger than a typical DC operational switching surge. Thus, in the case of pole to ground fault, the healthy pole failure risk appears to be low. However, further research is needed on higher voltages and polluted conditions.

Index Terms—Insulator, HVDC, Switching Impulse, Superimposition.

I. INTRODUCTION

HIGH Voltage Direct Current (HVDC) systems are increasingly being integrated into the power grid. The main drive for this is to harvest renewable resources like wind energy and solar radiation or to maximize the transmission capability of the power system between the areas of production and consumption of electricity. The development and implementation of such

Manuscript received February 11, 2020; revised April 27, 2020; accepted June 4, 2020. Date of publication June 22, 2020; date of current version March 24, 2021. This work was supported by the European Union's Horizon 2020 Marie Skłodowska-Curie program, under Grant 765585. Paper no. TPWRD-00220-2020. (Corresponding author: Davide Pinzan.)

Davide Pinzan, Manu A. Haddad, Mohammed El Amine Slama, Maurizio Albano, and Ronald T. Waters are with the Advanced High Voltage Engineering Research Centre, Cardiff University, Cardiff CF10 3AT, U.K. (e-mail: PinzanD@cardiff.ac.uk; Haddad@cardiff.ac.uk; SlamaME@cardiff.ac.uk; AlbanoM@cardiff.ac.uk; WatersRT@cardiff.ac.uk).

Fabio Branco and Helder Leite are with the High Voltage Laboratory, Department of Electrical and Computer Engineering, University of Porto, Porto 4099-002, Portugal (e-mail: fabiobranco@fe.up.pt; hleite@fe.up.pt).

Color versions of one or more of the figures in this article are available online at <https://ieeexplore.ieee.org>.

Digital Object Identifier 10.1109/TPWRD.2020.3003980

new technology bring new research challenges that need to be investigated. One of these challenges is to determine how outdoor insulators perform under various stress conditions. For example, when a pole to ground fault occurs on bipolar DC lines, the healthy pole is stressed by a slow transient overvoltage superimposed on the system DC voltage [1]–[4]. The same happens for the neutral conductor [5]. These superimposed overvoltages are similar to a Switching Impulse (SI) [5].

This paper aims at contributing to the understanding of the new problem by bringing new experimental data of tests operated on a composite insulator. These tests have been performed with positive and negative SI voltage, and negative SI voltage superimposed on negative direct voltage. A comparison between the two tests has been conducted to quantify the degradation of performance due to DC energization when switching impulse is superimposed and explore whether an indicative [6], [7] switching surge factor (SSF) of 1.5 can be safely withstood. SSF is defined as the ratio between the maximum switching surge voltage and maximum operating pole to ground voltage of the power system [8].

An analysis of the time to flashover with respect to the flashover voltage has also been performed to determine the possible relationship with the superimposition test. This analysis of the time to flashover is essential to HVDC systems control engineers to accurately simulate the instant of fault caused by switching surges.

This work will be of interest primarily to outdoor insulator technical experts and Standard Tests developers, HVDC protection engineers and scientists and, secondarily, to Transmission System Operators (TSOs).

II. BACKGROUND

A number of papers have been published on the characterization of outdoor insulation under HVDC, as reviewed in [9], [10], and under lightning impulse superimposed on direct voltage [11]. However, to the authors' knowledge, only Cortina's paper [12] and Watanabe's paper [13] describe the superimposition energization, which is carried out in this work. Cortina *et al.* [12] used a fixed amount of Salt Deposit Density (SDD), using rain on substation post insulators, glass cap-and-pin and composite long rod suspension insulators. Watanabe [13] investigated non-composite insulators under the dry condition only.

Despite the consistent deployment of DC outdoor insulation in industrial environments characterized by acid conductive

precipitation [9], such as eastern North America, Europe and eastern China [14], the dependence of flashover on rain conductivity has not been adequately studied under SI, and SI superimposed on direct voltage. This paper investigates this aspect through the measurement of flashover performance of composite insulators when rain is applied at different conductivities. For comparison purposes, the dry condition has been investigated too.

This voltage superimposition may cause an arc alongside the insulator, which should be avoided by the DC insulation coordination [8]. The flashover may occur in the case of substation vertical post insulators, overhead line horizontal tension, post, and cross-arm insulators. It may also occur alongside suspension line insulators if they are sufficiently short.

It is worth noting that Liao *et al.* [15] show results regarding the SI superimposition on DC voltage, but the authors consider the electric arc to occur across a uniform air medium (clear, open-air), not alongside the insulator. This assumption is valid for traditional high voltage towers equipped with suspension insulation. However, as stated in the examples above, there are cases where this hypothesis is not valid anymore.

III. EXPERIMENTAL SETUP

The laboratory layout, components and test specifications are described in this section. Two laboratory test arrangements were used in this program, depending on the presence of the DC power supply. For both arrangements, the rain tank and the rain nozzles have been employed at different water conductivities. In addition, the dry condition has been investigated.

Fig. 1 shows the vertical and horizontal test configurations of the test insulators as used in this work. The vertical arrangement was achieved by hanging the insulator from the metallic structure with a thick copper strip conductor. The horizontal was achieved fixing the insulator to the side of the metallic structure. The shortest distance between the high voltage energized rod and ground is set to be across the insulator, not across any other air gap. This is done to reproduce the electrical behavior of line tension, post and cross-arm insulators, and substation post insulators. The tested composite insulator is described in Fig. 2 and Table I.

To supply the high voltage waveshapes, the following equipment has been used: a Phenix 120 kV DC Hipot test set and 6 stages of a 12-stage Haefely SGS impulse voltage generator. To protect the DC source from the switching impulse, a 120 M Ω water resistor has been used. This resistor is constituted by a polyvinyl chloride (PVC) tube filled with distilled water. This allowed the DC source to stay part of the circuit during the switching impulse. To isolate the voltage divider from the DC source, a sphere gap was employed, with spheres diameter of 125 mm and separated by a gap of 25 mm.

The various tests carried out in this work are presented in Tables II and III, which show the requirements set by BS EN 60060-1:2010 Standard [16]. As can be seen in Tables II and

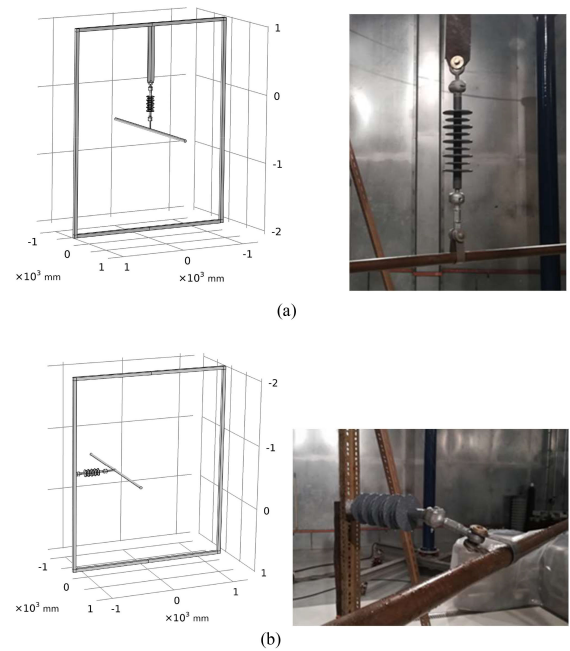


Fig. 1. Vertical and horizontal arrangement of the insulator. (a) Vertical test configuration. (b) Horizontal test configuration

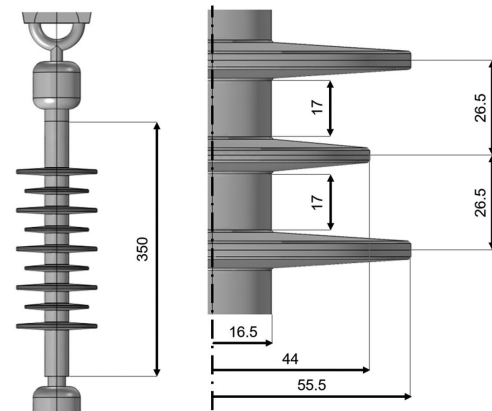


Fig. 2. Tested insulator. All units are in millimeters.

TABLE I
TEST INSULATOR DIMENSIONS

AD (mm)	CD (mm)	CF	Material of	
			Core	Umbrella
350	1047	3.0	Fiber glass	SiR ^a and EPDM ^a mix

AD = arcing distance, CD = creepage distance, CF = creepage factor.

^aSir = Silicone Rubber, EPDM = Ethylene Propylene Diene Monomer.

III, the interval ranges and values applied in our tests are more demanding than required, whenever possible.

TABLE II
SWITCHING IMPULSE TEST PARAMETERS

t_p (μ s)	t_h (μ s)	$\Delta U\%$	Impulses per group
Standard 250 \pm 50	Standard 2500 \pm 1500	Standard 1.5% - 3%	20
Applied 250 \pm 10	Applied 2500 \pm 50	Applied 2 %	

t_p = peak time, t_h = time to half.

TABLE III
RAIN TEST DATA

Rain rate (mm/min)	Application time (min)	Standard conductivity (μ S/cm)	Applied Conductivities (μ S/cm) (k Ω ·cm)
Vertical 1.5 \pm 0.5	≥ 15	100 \pm 15	σ_1 96.2 10.4
Horizontal 1.5 \pm 0.5			σ_2 160.8 6.2
			σ_3 354 2.8
			σ_4 527 1.9

For both configurations, the rain orientation was kept constant in front of the grounded metallic structure, at about 45° with respect to the floor.

IV. METHODOLOGY

A. The Rain Conductivity

As shown in Table III, a conductivity of 96.2 μ S/cm has been applied as requested by the standard [16]. However, many conductivities have been used to study the insulation performance in conductive rain conditions. One of the main molecules present in acid rain is sulfur dioxide [17]. However, using it to vary the test rain conductivity would affect the reliability of results, because it would evaporate during the test [18]. Therefore, to reproduce different conductivities, the following technique has been used. Different combinations of distilled water, aquifer water, and NaCl have been employed.

The first conductivity has been obtained by using distilled water only; the second has been obtained by mixing distilled and tap water; the third is the laboratory aquifer water conductivity; and the fourth is the aquifer water conductivity when NaCl is dissolved in it. The quantities of the components have been adjusted in a way to obtain a uniform set of conductivities that would evenly describe the relationship between the flashover voltage and the conductivity of the wetting solution.

The choice of the conductivity interval has been inspired by a previous study [19], which investigated the AC flashover performance reduction due to an increase in rain conductivity. The study [19] had shown that, with respect to 71 μ S/cm (14 k Ω ·cm), a significant decrease in flashover performance would appear when the solution conductivity is greater than 100 μ S/cm (below 10 k Ω ·cm) and would be drastically reduced by 50% at 500 μ S/cm (2 k Ω ·cm).

B. Selection of Direct Voltage Magnitude

The direct voltage magnitude has been selected for the insulator under the hypothesis of high NSDD and ESDD on the field, both of 0.6 mg/cm². From a previous paper [20], it is possible to derive (1) for the direct voltage calculation. The calculated

direct voltage is a function of the insulator material, geometry, and hypothetical installation environment:

$$U = \frac{CD}{B \cdot C_D \cdot C_a \cdot \left[ESDD_{dc} \cdot K_C \cdot \left(\frac{NSDD_{dc}}{0.1} \right)^{\frac{0.106}{\alpha}} \cdot K_{CUR} \cdot K_D \cdot K_S \right]^\alpha} \quad (1)$$

$$= 16 \text{ (kV)}$$

To calculate the direct voltage value, the calculation of the average diameter of the insulator [21] is needed and gives in this case 60.725 mm. For brevity, the explanation of all remaining parameters is not included and can be found in [20].

C. Flashover Voltage Measurement

The applied direct voltage and current were measured at the source, by the Phenix supply. To measure the voltage impulse, the Haefely damped capacitive impulse divider has been used. To measure both DC and switching impulse components, a mixed divider would be the best option. However, the damped capacitive impulse divider has proven to be sufficient to accurately measure the impulse transient, which was causing the flashovers. A detailed explanation is provided here.

Immediately before the impulse trigger, the voltage across the test object is equal to the direct voltage applied by the DC source minus a small voltage drop (3% of 16 kV) along the portion of the circuit that connects the DC source to the insulator. At this instant, the voltage divider measures 0V. After the trigger, the sphere gap charges up to -70 kV in about 38 μ s and it breaks down at that voltage. Following the instant of sphere gap breakdown, the divider measures precisely the voltage across the insulator. Therefore, the voltage peak of a withstand case and the flashover voltage measured by the divider did not need to be summed with the DC component value.

To verify that the peak of the voltage superimposition lies in an expected interval, a gap can be used at the specimen location, and multiple tests are done. As the voltage superimposition remains the same for each test, the initially large gap distance is reduced. The interval in which the voltage peak lies is determined by two subsequent tests of opposite result, namely withstand and breakdown.

D. U_{50} and $\sigma_{tf}\%$ Calculation

According to [16], to calculate U_{50} , which is the prospective voltage value which has a 50% probability of producing a disruptive discharge on the test object, the up and down method has been followed for each case. All flashover or withstand voltages have been corrected according to the ambient pressure, humidity, and temperature. The U_{50} value has then been computed as shown in (2):

$$U_{50} = \frac{\sum_{i=1}^n U_i}{n} \quad (2)$$

where U_i is the flashover voltage or withstand peak voltage of each impulse and n is the number of impulses per case. In this work, n was 20 for every case.

The percent time to flashover standard deviation $\sigma_{tf}\%$ has also been calculated, with respect to the switching impulse peak

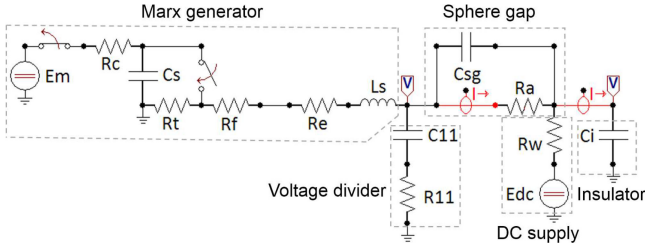


Fig. 3. EMTP/ATP circuit model of the experimental set-up.

TABLE IV
FULL DESCRIPTION OF THE CIRCUIT MODEL

Elements	Description	Magnitude
E_m	Marx generator voltage	Variable V
R_c	Resistor for capacitor charging	8400.6 Ω
C_s	Stage capacitor	0.6/6 μF
R_t	Impulse tail resistor	8400.6 Ω
R_f	Impulse front resistor	20.6 Ω
R_e	External water resistor	50 k Ω
L_s	Inductance due to how stage is configured	2.5.6 μH
C_{11}	Voltage divider high voltage capacitor	1200 pF
R_{11}	Voltage divider high voltage resistor	100 Ω
C_{sg}	Sphere gap capacitance - FEM calculated	0.325 pF
R_a	Current dependent arc resistance, by Toepler	(4)
k_t	Toepler formula constant	$0.5 \cdot 10^{-4}$ V-s/cm
D	Gap between spheres	2.5 cm
R_w	Protective water resistor, for DC supply	120 M Ω
E_{dc}	Direct voltage	16 kV
C_i	Insulator capacitance - FEM calculated	0.877 pF

time, as shown in (3)

$$\sigma_{t_f} \% = \frac{\sqrt{\frac{\sum_{j=1}^m [t_{f,j}(\mu\text{s}) - \bar{t}_f(\mu\text{s})]^2}{m-1}}}{250(\mu\text{s})} \cdot 100 \quad (3)$$

Where m , 10 statistically, is the number of flashovers per test case, $t_{f,j}$ is the time to flashover of each impulse, and \bar{t}_f is the average time to flashover per test case.

E. EMTP/ATP Simulation

An Electromagnetic Transient Program, EMTP/ATP, simulation has been carried out to analyze the transient characterized by the sphere gap breakdown and determine the voltage applied to the insulator. The calculation of the sphere gap and the insulator capacitances was performed in COMSOL Multiphysics. The simulation circuit is shown in Fig. 3. Table IV summarizes the parameters used for the circuit model.

Many current-variable resistance arc models are available in the literature [22]–[29]. As recommended in [30], the Toepler law [28] has been adopted, as (4) shows in Table IV.

$$R(i(t)) = \frac{k_t \cdot d}{\int_0^t i(t) dt} (\Omega) \quad (4)$$

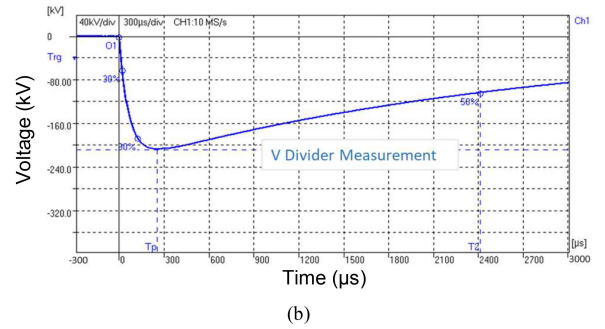
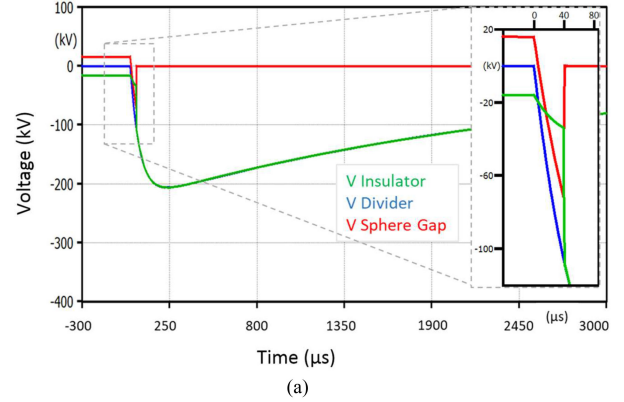


Fig. 4. (a) EMTP/ATP simulation results for the switching impulse superimposed on DC energization; (b) damped capacitive divider experimental measurement during the superimposition of the switching impulse and DC voltage obtained in the laboratory. (a) EMTP/ATP simulation results. (b) Voltage divider measurement

V. RESULTS AND DISCUSSION

A. Measurement Versus Simulation of Divider Voltage

The EMTP/ATP simulation results show the applied voltage on the insulator in Fig. 4(a) which allowed to observe the difference compared with the damped capacitive divider measurement shown in Fig. 4(b).

The divider-measured voltage and the insulator actual voltage differ by the sphere gap voltage. As Fig. 4 shows, the sphere gap is DC charged positively, despite the negative DC voltage. When the impulse generator is triggered, the sphere gap behaves first as a capacitance charging negatively and, when it breaks down at -70 kV [31], it follows the Toepler law [28] as a variable resistance arc, in parallel with the gas stray capacitance. Therefore, the voltage applied across the insulator differs from the Marx generator switching impulse. In fact, at first, the insulator is charged more slowly than it should because the sphere gap is also being charged negatively by the impulse. Then, when the sphere gap voltage collapses, a relatively high capacitive current is applied to the insulator. This current is high relatively to the time window considered in Fig. 4(a) and it causes a higher risk of puncture, compared to the risk of a slower switching impulse front.

The laboratory measurement agrees well with the simulation and confirms that the damped capacitive divider can measure a fast impulse voltage but cannot measure the DC component just

before the start of the impulse. Thus, the flashover and withstand voltages detected by the divider did not need to be added to the DC component.

B. Dry and Wet Flashover Under Switching Impulse Superimposed on Direct Voltage

In this work, the test program examined the performance of the outdoor insulator under different energizations, orientations, and rain conductivities. Three groups of results are presented: (a) positive switching impulse, (b) negative switching impulse and (c) negative switching impulse superimposed on negative DC energization. In addition to the wet tests, the dry condition has been included in the charts at 0 $\mu\text{S}/\text{cm}$. To visualize the results from the point of view of the U_{50} drop with respect to the dry case, (5) has been used.

$$1 - \text{drop} = 1 - \frac{U_{50,dry} - U_{50,wet,i}}{U_{50,dry}} \quad (p.u.) \quad (5)$$

Fig. 5(a), (b), and (c) show a decrease of performance when the rain is applied and when the conductivity is increased. This is true in every case with only one evident exception which is the positive horizontal flashover under the 96.2 $\mu\text{S}/\text{cm}$ rain. The test has been repeated to confirm this was not due to bad measurements. These results confirm the expected behavior of decreased performance when the insulators surface is wet and becomes more conductive, facilitating the discharge inception and propagation until flashover.

The insulator performance drops the most between the dry and the 96.2 $\mu\text{S}/\text{cm}$ rain conditions, when stressed with both the negative impulse with and without negative superimposed direct voltage. As can be seen in Fig. 5, beyond a rain conductivity of 160.8 $\mu\text{S}/\text{cm}$, very little decrease of the flashover is measured. The positive SI flashover of the vertical orientation chart shows the largest drop in breakdown voltage between the lowest rain conductivity and the next conductivity. Whereas, for the horizontal case, the positive impulse chart shows a variable behavior.

The minimum and thus most critical switching surge factor that the insulator is able to withstand is $172 \text{ kV} / 16 \text{ kV} = 10.8$, which is much larger than 1.5 [6]. Cortina *et al.* [12] have shown a minimum of $1500 \text{ kV} / 300 \text{ kV} = 6$. It follows that, in the absence of pollution accumulation, the arc span of the healthy pole insulators is not likely during the transient overvoltage due to pole to ground fault of a bipolar circuit, but the risk is higher [12] with increasing DC system voltage.

Fig. 5(a) and (b) show that the positive SI is more severe in the dry case. However, the same does not occur for the wet conditions. In some cases, the negative SI has proven to be more severe than the positive, and in other cases the difference is not evident. Thus, at these voltage levels, both positive and negative superimpositions need to be investigated. This paper contributes to the understanding of the phenomenon by investigating in detail the negative, as shown in Fig. 5(c).

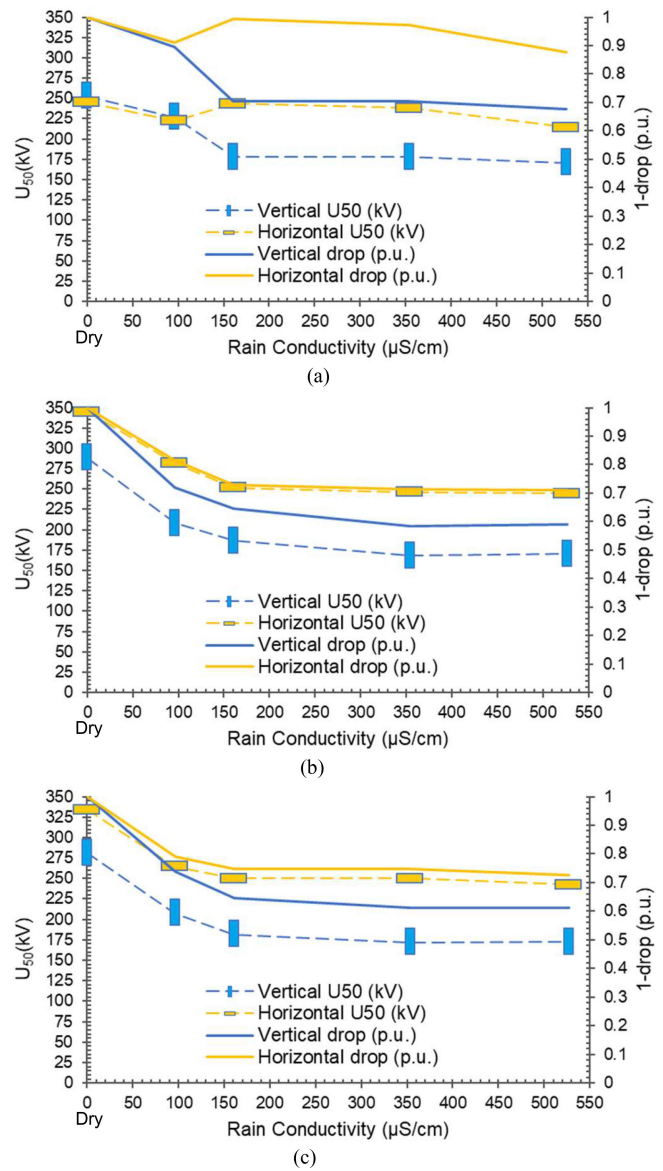


Fig. 5. On the left, the flashover voltage as a function of rain conductivity. On the right, the flashover drop, with respect to the dry condition, as a function of rain conductivity. Each chart includes the dry condition at 0 $\mu\text{S}/\text{cm}$. (a) Positive SI. (b) Negative SI. (c) Negative DC and negative SI

C. The Influence of Direct Voltage

To clarify the influence of the DC energization application before the SI on the flashover voltage, the chart of Fig. 6 gives the percentage of the flashover voltage drop due to the DC energization with respect to the DC voltage.

Compared with negative SI, the application of the negative DC pre-energization causes the largest performance drop in the dry and in the horizontal lowest rain conductivity cases; particularly, the biggest difference is found for the horizontal wet condition. In most cases, the direct voltage affects negatively the flashover performance, but with an unclear profile. Moreover, it needs to be noted that the DC is only 6.8% of the average impulse. A higher DC energization may have caused a larger degradation of performance.

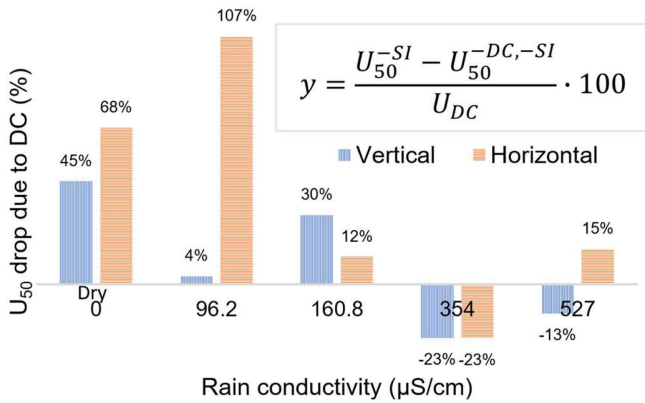


Fig. 6. The flashover voltage drop due to the DC energization normalized to 16 kV, which is the applied direct voltage, as a function of rain conductivity.

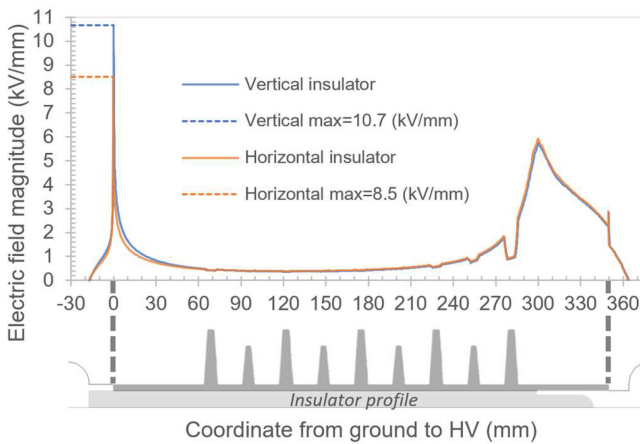


Fig. 7. Electric field magnitude along the creepage path of the insulator as a function of axis coordinate, in both orientations, with high voltage electrode at 288.230 kV.

D. Effect of Insulator Orientation on Flashover Voltage

The insulator shows a notably better performance when tested horizontally, except for the first two cases of positive switching impulse. The trend is attributed to the larger horizontal surface area and thus larger amount of deposited rain when the insulator is vertically oriented, and because the elongation of water droplets during their free fall is oriented vertically, facilitating the creation of an arc path in the vertical orientation. However, it was not obvious that the vertical arrangement would perform worse also in the dry case. Thus, the calculation of the electric field magnitude along the creepage path of the two arrangements has been carried out, as shown in Fig. 7.

Fig. 7 indicates the maximum electric field magnitude is located on the edge of the ground electrode for both orientations. In the vertical orientation, the maximum value is larger than that of the horizontal because the ground electrodes are different. In the vertical case, the copper strip conductor causes the equipotential lines to squeeze in the vicinity of the ground electrode, as Fig. 8 shows.

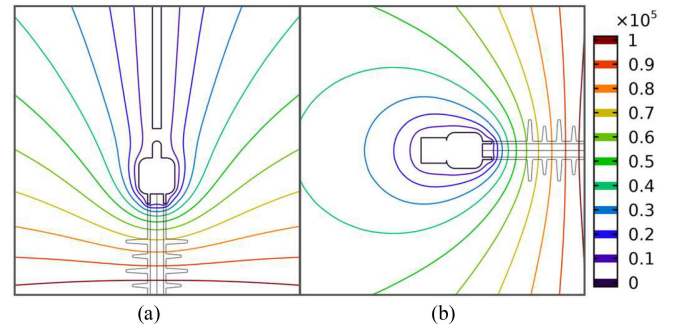


Fig. 8. Equipotential lines (V) in the vicinity of the ground electrode, when the high voltage electrode is at 288.230 kV. Each section view has been obtained with a cutting plane, which is vertical for (a), and horizontal for (b). (a) Vertical arrangement. (b) Horizontal arrangement.

TABLE V
TIME TO FLASHOVER DEVIATION, (+)SI

Rain Conductivity (μS/cm)	Vertical	σ_f %	Horizontal	σ_f %
Dry	19%	19%	35%	35%
96.2	18%	18%	35%	35%
160.8	119%	119%	264%	264%
354	56%	56%	22%	22%
527	32%	32%	47%	47%

If the ground electrodes were the same, the flashover voltage should be the same in the dry case. However, as can be seen in Fig. 5, regardless of the electrode configuration, the wet vertical cases drop, with respect to dry, more than the horizontal.

E. Time to Flashover

For the purpose of advancing protection control and power system fault simulations, Fig. 9 illustrates the time to flashover dependence on flashover voltage.

The results show a trend of decreasing time to flashover with increasing flashover voltage, as expected. Therefore, the vertical orientation takes longer to flashover. Moreover, the insulator time to flashover average increases in the presented order: positive impulse, negative impulse, negative impulse superimposed on negative DC. These results demonstrate that the protection and control are required to be faster when the impulse front voltage rate of change in time is large.

Also, if wet, the insulator takes more time to flashover.

The DC energization does not seem to cause any noticeable effect on the time to flashover.

Tables V, VI, and VII show the percent standard deviation of each time to flashover as defined in (3). No specific pattern has been identified.

By observing the average time to flashover of Fig. 9 and each associated standard deviation in Tables V, VI, and VII, it is

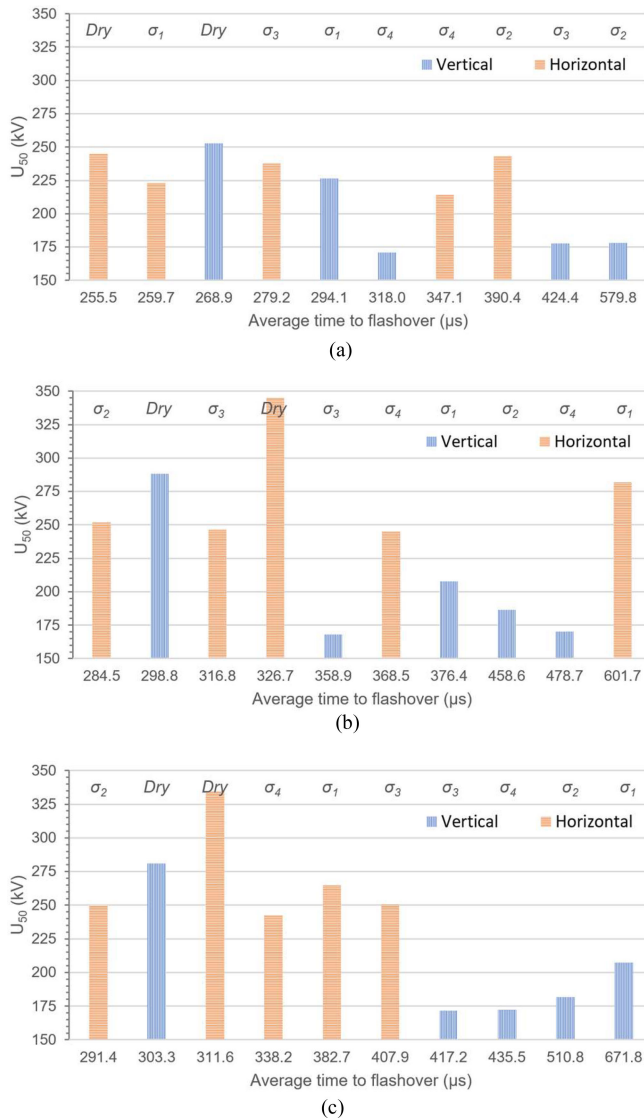


Fig. 9. Flashover voltage as a function of the average time to flashover. Each column is characterized at the top by its test condition. Legend of the rain conductivity σ is provided in TABLE III. (a) Positive SI. (b) Negative SI. (c) Negative DC and negative SI

possible to conclude that the vast majority of the individual times to flashover is greater than the SI peak time, namely 250 μs .

F. Flashover Voltage in Relation to Insulator Length

Evidence from other research show similar trends at higher voltages for longer insulators. Specifically, under the dry condition [12], [13], the flashover voltage of the negative superimposition is lower, and thus more severe, than the flashover voltage of the negative SI alone. Similarly, from the data provided by [12], the same trend can be identified for the wet condition.

The comparison of the available data provided by [12], [13], and this paper should be done cautiously. In fact, the studies are performed on insulators of different profiles, materials, and electrode configurations. Moreover, in these studies the direct

TABLE VI
TIME TO FLASHOVER DEVIATION, (-)SI

Rain Conductivity ($\mu S/cm$)	Vertical	$\sigma_f\%$	Horizontal	$\sigma_f\%$
Dry		43%		26%
96.2		37%		84%
160.8		53%		22%
354		38%		24%
527		59%		35%

TABLE VII
TIME TO FLASHOVER DEVIATION, (-)DC AND (-)SI

Rain Conductivity ($\mu S/cm$)	Vertical	$\sigma_f\%$	Horizontal	$\sigma_f\%$
Dry		34%		33%
96.2		236%		17%
160.8		37%		18%
354		62%		79%
527		61%		42%

voltage of each insulator length has not been selected with the same method.

VI. MAIN CONCLUSIONS

This paper has quantified experimentally the difference between the superimposition of a negative SI on a negative DC energization and a negative SI. Furthermore, it has assessed how rain and its conductivity value reduce the flashover performance of an outdoor composite insulator.

In most cases, the application of a negative SI superimposed on a negative direct voltage has been proven to affect the performance of the insulator more severely compared with the same negative SI on its own. In particular, the three cases which have been affected the most by direct voltage presence are the dry horizontal, the dry vertical, and the 96.2 $\mu S/cm$ rain horizontal cases.

However, the test object has always withstood switching impulses with peak values much greater than 1.5 times the applied direct voltage. Thus, at the studied voltage levels and in the absence of accumulated pollution, it is suggested that this type of flashover is not likely to happen in operation. To verify the same conclusion for pollution application and the positive superimposition, further investigations are needed.

In almost all cases, the horizontal orientation has proven to perform better than the vertical. Also, when wet, the horizontally oriented insulator has shown a performance drop ratio smaller than the vertical, with respect to the dry case.

It has been confirmed that the time to flashover shortens with increasing flashover voltage, but negligible role seems to be played by the direct voltage pre-energization.

ACKNOWLEDGMENT

The authors would like to thank Prof. Antonio Machado e Moura for his insights at the High Voltage Laboratory of University of Porto during winter 2018-2019.

REFERENCES

- [1] N. G. Hingorani, "Transient overvoltage on a bipolar HVDC overhead line caused by DC line faults," *IEEE Trans. Power Appar. Syst.*, vol. PAS-89, no. 4, pp. 592–610, Apr. 1970.
- [2] E. W. Kimbark, "Transient overvoltages caused by monopolar ground fault on bipolar DC line: Theory and simulation," *IEEE Trans. Power Appar. Syst.*, vol. PAS-89, no. 4, pp. 584–592, Apr. 1970.
- [3] D. J. Melvold, P. C. Odum, and J. J. Vithayathil, "Transient overvoltages on an HVDC bipolar line during monopolar line faults," *IEEE Trans. Power Appar. Syst.*, vol. 96, no. 2, pp. 591–601, Mar. 1977.
- [4] G. T. Wrate *et al.*, "Transient overvoltages on a three terminal DC transmission system due to monopolar ground faults," *IEEE Trans. Power Del.*, vol. 5, no. 2, pp. 1047–1053, Apr. 1990.
- [5] CIGRE WG B2.41, "Guide to the conversion on existing AC lines to DC operation. Technical Brochure 583," *CIGRE*, May 2014.
- [6] Oak Ridge National Laboratory (ORNL), "HVDC power transmission technology assessment," Oak Ridge, Tennessee 37831, Apr. 1997.
- [7] Electric Power Research Institute, EPRI, "AC-to-DC Power transmission line conversion," Nov. 2010.
- [8] National Electric Safety Code NESC, Part 1, Section 12, "C2-2017." *IEEE*, 2017.
- [9] CIGRE Task Force 33.04.01, "Polluted insulators: A review of current knowledge," CIGRE, Jun. 2000. [Online]. Available: <https://e-cigre.org/publication/158-polluted-insulators--a-review-of-current-knowledge>. Accessed: Jun. 05, 2018.
- [10] CIGRE Working Group C4.303, "Outdoor insulation in polluted conditions: Guidelines for selection and dimensioning - PART 2: THE DC CASE," CIGRE, Dec. 2012. [Online]. Available: <https://e-cigre.org/publication/518-outdoor-insulation-in-polluted-conditionsguidelines-for-selection-and-dimensioning---part-2-the-dc-case>. Accessed: Jul. 24, 2018.
- [11] S. K. Shifidi, H. J. Vermeulen, J. P. Holtzhausen, and P. Pieterse, "Impulse testing of a polluted insulator with a DC bias voltage," in *Proc. 16th Int. Symp. High Voltage Eng.*, Cape Town, South Africa, 2009, Paper C-4, pp. 1–5.
- [12] R. Cortina, G. Marrone, A. Pignini, L. Thione, W. Petrusch, and M. P. Verma, "Study of the dielectric strength of external insulation of HVDC systems and application to design and testing," presented at the *Int. Conf. Large High Voltage Electric Syst.*, 1984.
- [13] Y. Watanabe, "Influence of preexisting dc voltage on switching surge flashover characteristics," *IEEE Trans. Power Appar. Syst.*, vol. PAS-87, no. 4, pp. 964–969, Apr. 1968.
- [14] H. Rodhe, F. Dentener, and M. Schulz, "The global distribution of acidifying wet deposition," *Environ. Sci. Technol.*, vol. 36, no. 20, pp. 4382–4388, 2002, doi: [10.1021/es020057g](https://doi.org/10.1021/es020057g).
- [15] W. Liao, G. Cui, and Z. Sun, "Flashover tests on air gap of ± 800 kV DC transmission line under composite DC and switching impulse voltage," *IEEE Trans. Dielectr. Electr. Insul.*, vol. 21, no. 5, pp. 2095–2101, Oct. 2014, doi: [10.1109/TDEI.2014.004003](https://doi.org/10.1109/TDEI.2014.004003).
- [16] IEC/TC 42, *BS EN 60060-1 High Voltage test techniques. Part 1: General definitions and test requirements*, BSI Standards, 2010.
- [17] G. E. Likens and T. J. Butler, "Acid rain: Causes, consequences, and recovery in terrestrial, aquatic, and human systems," in *Encyclopedia of the Anthropocene*, D. A. Dellasala and M. I. Goldstein, Eds., Oxford: Elsevier, 2018, pp. 23–31.
- [18] Lightning and Insulator Subcommittee, "Application of insulators in a contaminated environment," *IEEE Trans. Power Appar. Syst.*, vol. PAS-98, no. 5, pp. 1676–1695, Sep. 1979.
- [19] T. Fujimura and K. Naito, "Electrical phenomena and high voltage insulators," in *Proc. Int. Symp. Ceramics Held at Bangalore*, Nov. 1982, pp. 1.04-1–1.04-15.
- [20] D. Pinzan, M. E. A. Slama, O. Cwikowski, and M. A. Haddad, "Insulation solutions for HVAC to HVDC conversion of a high voltage transmission overhead line: The L7 tower case study," in *Proc. 21st Int. Symp. High Voltage Eng.*, Budapest, Hungary, 2019, pp. 1359–1371.
- [21] BSI British Standards, "IEC/TS 60815-2:2008," 2008.
- [22] S. I. Barannik, S. B. Vasserman, and A. N. Lukin, "Resistance and inductance of a gas arc," *Sov. Phys. Tech. Phys.*, vol. 9, no. 11, pp. 1449–1453, 1975.
- [23] G. M. Gomcharenko and I. N. Romanenko, "Discharge channel in Helium at 100 atm and in Air," *Sov. Phys. Tech. Phys.*, vol. 15, pp. 1990–1995, Jun. 1971.
- [24] I. V. Dementik, "Resistance of a xenon plasma in a large flash lamp," *Sov. Phys. Tech. Phys.*, vol. 13, pp. 829–832, Dec. 1968.
- [25] M. J. Kushner, W. D. Kimura, and S. R. Byron, "Arc resistance of laser-triggered spark gaps," *J. Appl. Phys.*, vol. 58, no. 5, pp. 1744–1751, 1985, doi: [10.1063/1.336023](https://doi.org/10.1063/1.336023).
- [26] M. M. Popovic, "Investigation of the beginning of high current discharges in pulsed arcs," presented at the *Int. Conf. Gaseous Discharges*, 1974, pp. 32–36.
- [27] R. Rompe and W. Weizel, "Über das toeplersche funkengesetz," *Z. Für Phys.*, vol. 122, no. 9–12, pp. 636–639, 1944, doi: [10.1007/BF01330625](https://doi.org/10.1007/BF01330625).
- [28] M. Toepler, "Zur kenntnis der gesetz der gleitfunkenbildung," *Annu. Phys.*, vol. 326, no. 12, pp. 193–222, 1906.
- [29] A. E. Vlastos, "The resistance of sparks," *J. Appl. Phys.*, vol. 43, pp. 1987–1989, Apr. 1972.
- [30] J. Kuffel and P. Kuffel, "Operation, design and construction of impulse generators," in *High Voltage Engineering Fundamentals*, 2nd ed., Newnes, 2000.
- [31] Technical Committee PEL/42, "BS EN 60052:2002. Voltage measurement by means of standard air gaps," *BSI Standards*, 2002. [Online]. Available: <https://webstore.iec.ch/>. Accessed: Jul. 04, 2019.



Davide Pinzan (Member, IEEE) received the B.S. degree in energy engineering and the M.S. degree in electrical engineering from the University of Padua, Italy, in 2015 and 2017. In 2017, he was a Freelance Scholar for the Collaborative Intelligent Infrastructure of Florida State University, USA. Since 2018, as a member of the EU funded InnoDC project, he has been a Marie Curie Ph.D. Researcher at Cardiff University, UK. In 2019 he collaborated with the University of Porto, and with the UHVDC Test Base of China Electric Power Research Institute. Mr. Pinzan is a CIGRE student member since 2018.



Fábio Branco received the M.S. degree in electrical and computer engineering from the University of Porto (FEUP), Portugal, in 2015. Since 2016, he has been part of FEUP High Voltage Laboratory team. He develops the research activity in the field of high voltage. He provides support in the courses of high voltage techniques, and chemistry, materials and processes. He also acts as Coordinator for the M.S. theses developed at FEUP High Voltage Laboratory. In 2018 he started working as a Researcher in the GreenEst project, in partnership with EFACEC, and REN.



Manu A. Haddad (Member, IEEE) received the first degree in electrical engineering in 1985 and then a Ph.D. degree in high voltage engineering in 1990. He is now a Professor at Cardiff University. His research interests are in overvoltage protection, insulation systems, insulation coordination and earthing systems. He has published an IET-power series book on "Advances in High Voltage Engineering." He is a member of CIGRE working groups and a member of BSI PEL1/2, IEC TC37. He serves on the scientific committees of several international conferences. Prof. Haddad is a Fellow of the IET and a Fellow of the Learned Society of Wales.



Mohammed El Amine Slama (Member, IEEE) is currently Researcher with the Advanced High Voltage Engineering Centre of Cardiff University. He was previously Researcher at SuperGrid Institute, France, in collaboration with General Electric Grid-Solutions and Ecole Centrale de Lyon (2014-2017). He was Assistant Professor at the University of Sciences and Technology of Oran, Algeria, and Researcher at the “Laboratoire de Génie Electrique d’Oran” where he was member of High Voltage and Electrical Field Group since 2004. In 2008, he joined the Dielectric Materials and High Voltage Group at AMPERE Lab, CNRS in Ecole Centrale de Lyon, France, where he finalized the Doctorate thesis and was an Associate Professor at the University of Lyon 1 from 2010 to 2011. His main research interests include HVAC and HVDC outdoor insulation, GIS and GIL insulation, high voltage engineering, dielectrics and electrical insulation, HV power system protection and grounding. He is author/co-author of more than 80 scientific papers and technical reports.



Ronald T. Waters received the Ph.D. degree from the University of Wales, Swansea in 1954. He researched at AEI, Aldermaston, UK with teams on nuclear fusion, high speed photography, electron microscopy and high voltage technology. From 1963, his university work at Cardiff initiated international collaborations in high voltage engineering and gaseous breakdown, including participation with the European Les Renardieres Group on UHV phenomena. He has been closely associated since 1972 with the biennial International Symposium on high voltage engineering of which he is a Steering Committee member. He is a Fellow of IET (formerly IEE, UK) and is now Emeritus Professor at Cardiff University.



Maurizio Albano received the 5-year degree (M.Eng.) in 1999 and then the Ph.D. degree in electrical engineering from the University of Padova, Italy in 2003. In 2006 he joined the Advanced High Voltage Engineering Research Centre at Cardiff and is now Lecturer at Cardiff University. He is a Member of IET and IEEE. His present fields of research are insulation co-ordination, electromagnetic fields computation, air insulated compact substations and overhead line insulator design.



Helder Leite (Member, IEEE) received the degree in electrical engineering from the University of Porto, Portugal, and the Ph.D. degree in electrical engineering from the University of Manchester, Manchester, U.K., in 2000 and 2004, respectively. He has been a Lecturer with the University of Porto since 2005. His research interests include power system digitalization, power system protection and control for flexible and sustainable electric power systems.